Penny-shaped crack propagation in spallation of Zr-BMGs

Z. Ling[1,a], X. Huang[2], and L.H. Dai[1]

[1] LNM, Institute of Mechanics, Chinese Academy of Sciences, Beijing 100190, PR China
[2] Institute of Systems Engineering, China Academy of Engineering Physics, Mianyang 621900, PR China

Abstract. Typical penny-shaped microcracks at their propagating in spallation of Zr-based bulk metallic glass (Zr-BMG) samples were captured by a specially designed plate impact technique. Based on the morphology and stress environment of the microcrack, a damaged zone or propagation zone around the crack tips, similar to the cohesive zone in classical fracture theories, is applied. Especially the scale of such a damaged zone represents a scale of the crack propagation. Its fast propagation would quickly bring a longer crack or cause cracks coalesce to form another longer one. The estimated propagation scales of microcracks are reasonable compared with what occurred in the Zr-BMG samples.

1. Introduction

Spallation in bulk metallic glasses (BMGs) is an important dynamic fracture under tensile pulse in uniaxial strain condition [1]. In contrast to the shear-sensitive fractures in BMGs under tensile stress in uniaxial stress condition [2,3], the spallation is controlled by hydro-static tension stresses. Therefore, spallation fractures take place in a plane of the maximum tensile stress, perpendicular to the tensile direction [1]. Spallation in BMGs is finally attributed to microdamage evolution occurred in a narrow layer where tensile stress amplitude reaches to its maximum. The narrow layer, alike a shear band in BMGs [4,5] supplies a hydro-tensile stress environment for microdamage nucleation, propagation and coalescence.

The spallation behavior of BMGs has been investigated according to spallation strength, spallation setup as well as microdamage evolution [6–9]. In the literatures on the spallation behavior in BMGs, little information exists concerning the microdamage nucleation, growth and coalescence of spallation [8]. Studies on microdamage evolution of Zr-based bulk metallic glasses' (Zr-BMG) spallation exhibited that, as having a unique amorphous structure or disorder atomic structure, Zr-BMG's microdamage evolution of spallation seems to be unlike the evolution of traditional crystalline metals. In particular, in the Zr-BMG samples the whole microdamage evolution, including nucleation, growth and coalescence, would take 10^2ns [8]. The microdamages in the material are microvoids in the size of 10^{0-1}nm [8], $10^{1\sim2}$nm [10] and 10^3 nm, in their respective to nucleation, growth and coalescence. Obviously, the microvoids' scale grows about 10^{1-2}nm during the growth process of 100 ns. This scale and duration are several orders smaller than those of traditional crystalline materials' microdamage evolution [1]. In this case, for further studies of microvoid evolution of spallation in the BMGs, it is extremely important to obtain accurate data for the voids and cracks during the evolution of 10^2 ns in the materials [1].

Plate-impact technique is an effective method to capture the evolution of microdamage of spallation in laboratories. This technique provides an experimental configuration of uniaxial tensile strain and a tensile hydro-static stress pulse. Especially, by controlling tensile stress amplitude and its duration in the technique, one can make microdamage at different evolution stage to be "frozen" in the samples [1] for further study. Recently, a plate-impact technique with specially designed flyers has been developed [11] to efficiently capture information of microdamage evolution of a 10^2ns duration in Zr-BMG samples. By this technique, mcrocracks of 10^{2-3}nm were "frozen" in the samples. In this paper, an investigation to the microcrack propagation occurred in Zr-BMGs under the plate impact is presented based on classical fracture theories.

2. Microdamage evolution experiments

2.1. Material and plate impact experiment

Spallation microdamage evolution tests were performed with a 101 mm single-stage light gas gun. To study microdamage evolution of a 10^2ns duration in Zr-BMGs, the short-multi-stress pulse technique was applied. In the plate-impact experiments, specially designed double-flyers were employed [11]. Figure 1 is a schematic of the specially designed apparatus, where three BMG samples are targeted by the three sets of double-flyers with gaps of varied sizes, so that microdamage in different stress durations, under the same stress amplitude, could be "frozen in" the BMG samples. The details of experimental implementation and the double-flyers technique can be referred to the paper [11].

The material applied in current experiments was $Zr_{41.2}Ti_{13.8}Cu_{12.5}Ni_{10}Be_{22.5}$ [Vit.1]. Table 1 presents mechanical properties of Zr-BMG, where ρ is density; E elastic modulus and E_L lateral elastic modulus; v Poisson's
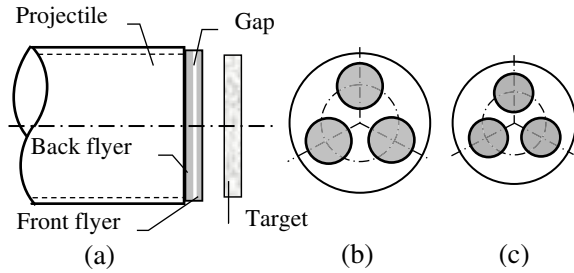
[a] Corresponding author: lingz@lnm.imech.ac.cn

Figure 1. A schematic of the special designed plate impact apparatus, (a) Plate impact apparatus with the specially designed double flyers; (b) Impactor and (c) Target.

Table 1. Mechanical properties of the Zr-BMG samples.

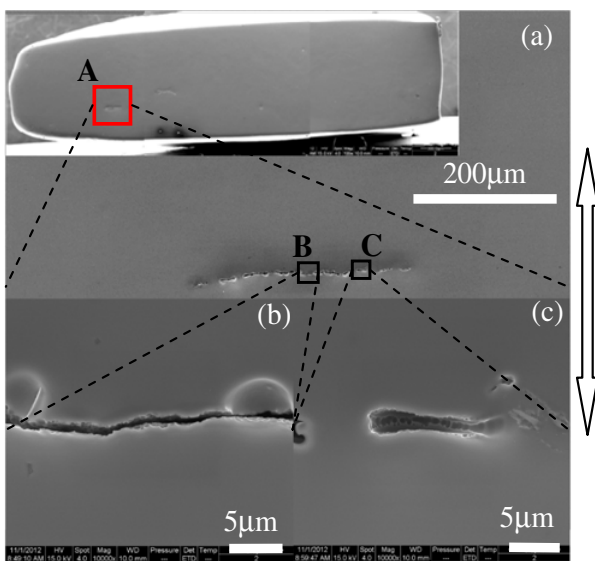| Materials	ρ (kg/m)^3	E(GPa)	E_L(GPa)	v	c_L(m/s)
Zr-BMG	6125	98.6	160	0.36	5182

Figure 2. Close-up observations of a part of the cross-section of a sample (σ 3.2 GPa, $\Delta t = 250$ ns), where (a) details of zone-A in the cross-section; (b) an enlarged show of zone-B and (c) zone-C. The arrow is along the loading direction.

ratio; c_L longitudinal wave speed [12]. After the impact experiments were performed, samples were recovered and sectioned to observe the induced microdamage. Each of the tested samples was cut along its diameter and then the cut-section was polished carefully. A scratch-free cross-section of the samples was obtained after being etched [3] for microscopic examination under higher magnification.

2.2. Micro-observations

Figure 2 presents typical micrographs of a partial cross-section of one microdamaged sample under a stress duration of 250 ns with stress amplitude of 3.2 GPa. As shown in the insert, under the given stresses with duration of 250 ns, strip-like concave regions have appeared in the sample. The strip-like concave regions have been verified as microdamage regions, 10^2 μm in length and parallel to each other. In particular they are perpendicular to the loading direction and located at where maximum tensile

stress is [11]. Meanwhile, no any other strip-like region can be seen on the section, either near by or far from the microdamage regions along the loading direction.

Figure 2a is an enlarged image of zone-A in the inserted square. The strip-like microdamage region consists of several disconnected micro-flaws. The longest flaw is about 150 μm with the others' length varied about 10–30 μm (Fig. 2a). Such micro-flaws are distributed along a strip located in the layer or plane of the maximum tensile stress, perpendicular to the impact direction.

Figure 2b is an enlarged show of zone-B marked in Fig. 2a, a part of a 150 μm crack, almost perpendicular to the loading direction. Part of the crack is slightly curvilinear, inferring the long crack may be formed by coalescence of several short cracks of 10^{0-1} μm.

Figure 2c is a detail of zone-C in the square in Fig. 2a. This is a crack with a length of 10 μm. Dimples of 10^{2-3} nm, without any tortuous, distributed along the internal edge of the crack. A few dimples of 10^2 nm can be seen on the upper and lower surfaces of the crack. The crack is obviously a typical penny-shaped crack located at where the maximum tensile stress is. Especially, the crack's tips are blunt and dimples of 2 μm are visible at the rim of one tip (Fig. 2c).

The penny-shaped crack shown in Fig. 2c is a typical microcrack in samples under plate impact loading [1], resulted from development of micro-damages. Previous researches on spallation of Zr-BMGs illustrates that microdamamges of the materials under hydro-static tension are microvoids with initial nucleation size of 10^0 nm [8]. Then tiny microvoids would grow up or coalesce to form larger voids, say 10^{1-3} nm and so on [10] and finally to leave dimples of 10^0 μm in the spallation morphology [8,9]. The penny-shaped crack of 10^1 μm in Fig. 2c seems not to be formed by microvoids' growth and coalesce only. The dimples of 10^2 nm along the crack's internal edge and those of dimples of 10^0 μm on the crack's blunt tips suggest that the penny-shaped crack would propagate after the crack's initial formation. To understand what observed in experiments, an investigation is presented in the following section to show how such a penny-shaped crack, like what in Fig. 2c, propagates under a given stress environment.

3. Penny-shaped crack's propagation

The given stress environment of a Zr-BMG sample under plate impact is uniaxial strain, that is, assuming loading direction is along z-axis,

$$\varepsilon_z \neq 0, \varepsilon_r = \varepsilon_\theta = 0 \tag{1}$$

where z, r and θ denote directions along thickness, radius and tangential direction of the sample, respectively. Stresses corresponding to the uniaxial strain are

$$\sigma_z = (K + \tfrac{4}{3}G)\varepsilon_z = E_L\varepsilon_z$$
$$\sigma_r = \sigma_\theta = \tfrac{v}{1-v}\sigma_z \tag{2}$$

where K, G and v are bulk modulus, shear modulus and Poisson's ratio; E_L is lateral elastic modulus, which is always higher than the elastic modulus. In the current case,
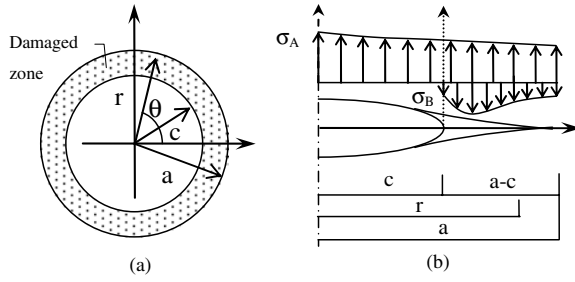
Figure 3. Schematic of a penny-shaped crack, (a) an overlook of the crack, where the shadow is damaged zone at rim of the crack; (b) stresses in the rim and surfaces of the crack.

Figure 4. Plots of $\frac{s}{c} \sim \frac{\sigma_A}{\sigma_B}$ shown as Eq. (7).

samples are under hydrostatic tension with a maximum tensile stress of 3.2 GPa, less than Zr-BMGs' Ugoniot Elastic Limit 6.7 GPa [12]. Therefore, the following investigations are quasi-static elastic.

3.1. Damaged zone

As shown in Fig. 2c, the penny-shaped crack is isolated and no any other visible microdamage clutters around its upper and lower surfaces, except for those at its bilateral with distances greater than 5 μm. This suggests that the crack's forming and propagating are in the layer or plane of the maximum tensile stress without being disturbed by other micro-damages or -cracks. It is worth noticing that, the penny-shaped crack is propagating under the tensile stress of 3.2 GPa within 250 ns, a stress environment of fixed stress amplitude within a given duration. Hence the current crack propagation in the short stress duration is approximately quasi-static. In such a case, an isolated crack's propagation can be described by classical fracture theories.

In these fracture theories, a crack with blunt tips illustrates that the stresses at the tip of the crack are limited, inferring at front of the crack's tip a small cohesive zone, compared with the crack's size [13,14]. The morphology and stress environment of the penny-shaped crack shown in Fig. 2c, suggest that a damaged zone or propagation zone, analogous to the cohesive zone above, is at the front of the crack's tip. In contrast to the case of the small cohesive zone [13,14], the current case is of a large-scale involving in micro-damaging [1], since microvoids have been observed further away around the microcrack tip (Fig. 2c).

Figure 3 is a schematic of a penny-shaped crack and its rim [15]. Figure 3a is an overlook of the crack, where the shadow represents a latent damaged zone at the rim of the crack. In the figure, c is radius of the crack, s size of the damaged zone, and a total length of the crack and its damaged zone, $a = c + s$. Figure 3b shows stress distributions around the crack, in which σ_A is stress acting on the surface $a = c + s$ to cause the crack's opening along the tension direction; σ_B is the cohesive stress acting partially over the crack's surface in the damaged zone attempting to close up the crack, in the direction opposite the tension. Stress σ_B also represents material resistance to microstructure evolution, intrinsic defects motion or microvoids nucleation in the region over the damaged zone [14,15]. Both stresses σ_A and σ_B are supposed to
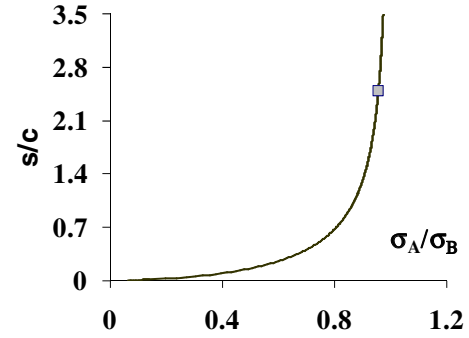
be uniform in the affected region. In addition, as being a hydro-static tension, the crack is subjected to other two stresses σ_r and σ_θ. Apparently, these two stresses are acting in planes perpendicular to the crack's opening direction, so do not contribute to the opening.

The stress intensity factor of the total stress on the tip of the penny-shaped crack is[14]

$$K_T = K_A - K_B \qquad (3)$$

where K_A is contributed by the stress σ_A applied on $a = c + s$, K_B is by the stress σ_B acted on $s = a - c$. For a 3-D penny-shaped crack, one has

$$K_A = \frac{\sigma_A \sqrt{a}}{\pi} \qquad (4)$$

$$K_B = \frac{\sigma_B \sqrt{a}}{\pi} \left(1 - \frac{c^2}{a^2}\right)^{1/2}. \qquad (5)$$

A crack's blunt tip infers stresses on the tip are limited, only valid when $K_A = K_B$. Thus,

$$\frac{\sigma_A \sqrt{a}}{\pi} = \frac{\sigma_B \sqrt{a}}{\pi} \left(1 - \frac{c^2}{a^2}\right)^{1/2} \qquad (6)$$

Noticing $a = c + s$, this leads to

$$\frac{s}{c} = \left[1 - \left(\frac{\sigma_A}{\sigma_B}\right)^2\right]^{-1/2} - 1 \qquad (7)$$

As shown in Eq. (7), a penny-shaped crack's damaged zone is dependent on the crack's length and the loading on the crack as well as the cohesive stresses. Moreover in current case, once $K_A > K_B$, the crack propagates along where the damaged zone is under a given stress environment. The scale of the damage zone s also represents a propagation scale of the crack. In other words, a current crack of c would grow up to become a new one in the scale of a, thereupon $s = a - c$ corresponds to the propagation scale of the current crack.

Figure 4 is a plot of Eq. (7), between s/c and $\frac{\sigma_A}{\sigma_B}$. Clearly, stresses in the rim of the crack are always higher than that on the crack surface, i.e. $\sigma_A < \sigma_B$. However, with increasing $\frac{\sigma_A}{\sigma_B}$, s/c varies. While $\sigma_A \leq \frac{\sqrt{3}}{2}\sigma_B$, $s/c < 1$, which illustrates that the scale of damaged zone increases but is still less than that of the crack. Obviously this process corresponds to a slow propagation of the crack.
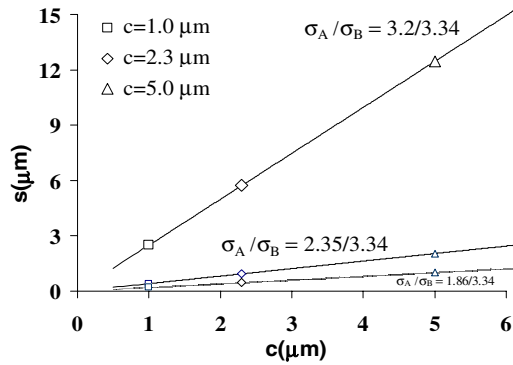
Figure 5. Plots of $s \sim c$ for the current Zr-BMGs.

After $\sigma_A > \frac{\sqrt{3}}{2}\sigma_B$, $s/c > 1$, the scale of the damaged zone increases, always greater than that of the crack. In particular, with $\sigma_A \to \sigma_B$, a little incremental in $\frac{\sigma_A}{\sigma_B}$ would lead to the damaged zone to develop fast. Thereby this of course corresponds to the fast propagation of the crack.

Further understand to this procedure would require more details about the current microcrack and its stress environment.

3.2. Propagation scale

As stated above, the scale of the damaged zone s also represents a scale of the crack propagated, verified by the current experimental data. The maximum tensile stress in current samples is 3.2 GPa. Under this tensile stress, resultant penny-shaped crack shown in Fig. 2c is about 5 μm radius and at the crack tip (right side) a dimple pattern about 1 μm radius (Fig. 2c) appears. The dimple pattern at the crack tip hints that the stress amplitude in the zone is 3.34 GPa, the critical stress of a microvoid in its critical size [10]. So $\frac{\sigma_A}{\sigma_B} = \frac{3.2}{3.34}$ is chosen for the current case of the crack's fast propagation, as shown in the square in Fig. 4.

In addition, there is no any other visible microdamage around the microcrack on both upper and lower surfaces in this sample, even if under high magnifications (Fig. 2). Nevertheless, as being demonstrated in previous studies, the microvoids nucleated size is about 10^{0-1} nm, too tiny to be visible with currently available microscopic instruments [8,9]. The loading stress of 3.2 GPa is obviously higher than the nucleation stress of 2.35 GPa [8] and static tensile strength of Zr-BMGs, 1.86 GPa [16]. Therefore in this case, probably some tiny microvoids have been nucleated, especially around the crack's upper or lower surfaces. Therefore two stresses of 2.35 GPa and 1.86 GPa are also supposed on the crack surfaces.

Figure 5 exhibits plots of $s \sim c$ of current Zr-BMG samples corresponding to the above stresses. As exhibiting, $\frac{\sigma_A}{\sigma_B} = \frac{3.2}{3.34}$ represents the current case and the other two, $\frac{\sigma_A}{\sigma_B} = \frac{2.35}{3.34}$ and $\frac{\sigma_A}{\sigma_B} = \frac{1.86}{3.34}$ are cases of microvoid nucleation and static tensile strength of this Zr-BMG, respectively. Three symbols represent the current crack size (radius) $c = 5 \mu$m (Fig. 2c); nucleated microvoid's critical size (radius) $c = 2.3 \mu$m [12] as well as the maximum void size at the crack tip in Fig. 2c $c = 1 \mu$m.

The line with a tangent of 3.2/3.34 in Fig. 5 corresponds to the current case. In this case, $s > c$, that is, the damaged zone develops faster than the crack, or the scale of a crack propagation is greater than that of the crack. While a crack is very short, say $c = 1$–2 μm, the damaged zone is about 2–5 μm and a resultant crack would be of 3–7 μm in radius. This is almost as the same as of the crack in Fig. 2c, that is, a 5 μm radius crack would be developed from propagation of a 1–2 μm radius crack. While a crack becomes longer, say 5 μm in radius, the length of its damaged zone would be 2.5 times of the current crack. This indicates that the crack propagates exceeding 17 μm radius and a resultant crack is to be 30 μm in its length. This seems to be beyond what was observed in Fig. 2c, whereas microcracks of 20–30 μm appeared in the same sample (see Fig. 2a). This also illustrates that a crack of 30 μm in length is probably resulted from the propagation of another crack of 5 μm in radius, like that in Fig. 2c.

In Fig. 5, crack propagation along the line with a tangent of 2.35/3.34 is the case of microvoids nucleated around the upper and lower surfaces of the crack. It is a linear dependence of the damaged zone and the crack. Compared with the fast propagating in the case of 3.2/3.34, the crack's damaged zone develops much slower than the crack, i.e. $s/c < 1$. Especially, the estimated damaged zone of the current crack of 5 μm radius is about 2.0 μm, less than the distance between the crack and its adjacent crack shown in Fig. 2c. A reasonable explanation is probably that, the nucleated microvoids around the crack caused stress relaxation, resisting or slowing the development of the damaged zone.

The bottom line with a tangent of 1.86/3.34 in Fig. 5 is the case of that the material around the crack is at its static tensile strength. Clearly, along this line, one possible damaged zone develops slower than those of 2.35/3.34 and 3.2/3.34. Hence, for a given crack under the given stress environment, the crack propagating may be always limited on local, unless increasing the stress amplitude or extending the stress duration.

3.3. Discussions

Based on the morphology and stress environment of a penny-shaped crack in Zr-BMG samples, a simplifying approximation to the damaged zone around the crack tips is applied. Actually, the latent damaged zone is resulted from nucleation, growth, and coalescence of millions of tiny voids in nano- or micro-scales [1]. Therefore the damaged zone's scale represents the scale of crack propagation scale. Following this way, further understanding of the damaged zone's developing is presented as following:

As being obvious in Fig. 5, there are two areas, fast crack (3.2/3.34) propagation and slow propagation (2.35/3.34, 1.86/3.34). In the fast propagation, along the line with a tangent of 3.2/3.34, the crack's propagation zone is fast increased so that it will meet with another crack's propagation zone. In this case, linking or coalescing between two adjacent cracks develops readily, or more adjacent cracks link each other simultaneously. This has been verified by the crack of 150 μm exhibited

in Fig. 2a, formed as coalescence of several cracks of $10^1\,\mu$m distributed in the same layer. Furthermore, in view of microdamage evolution, the crack in Fig. 2c probably was formed later compared to other cracks [1]. While this crack just grows to $5\,\mu$m radius from 1–$2\,\mu$m, the other cracks have been coalesced to form a longer one, say $150\,\mu$m (Fig. 2a).

Meanwhile, in the slow propagation (the line of 2.35/3.34), the crack propagation is always less than the current crack, implying that cracks' linking may not take place between two adjacent cracks. Compared with those in the fast propagation (the line of 3.2/3.34), a crack in the same size in slow propagation probably is always isolated, like that in Fig. 2c. Evidently, cracks under or below the stress of 2.35 GPa would not develop to be linked and form longer cracks.

This understanding of the fast propagation (3.2/3.34) and slow propagation (2.35/3.34, 1.86/3.34) of a current crack is in fact consistent with the understanding of critical criteria of spallation [17]. It is well known that spallation is resulted from microcracks nucleation, growth and coalescence under a given stress amplitude within a stress duration. If the applied stress amplitude is high enough, the resultant internal microcracks would propagate and link in sudden so that spallation occurs. However, in case of a low stress amplitude, possible nucleated microcracks would propagate too slowly to coalesce, even if the stress duration maintains longer. Hence, in case of these isolated microcracks, spallation could not be completed due to lack of cracks' coalescing or linking.

4. Conclusions

Propagation of a penny-shaped microcrack in Zr-BMG samples under uniaxial strain or hydrostatic tension has been described. The followings are deduced:

1. Typical penny-shaped microcrack propagation was "frozen" in Zr-BMG sample by a specially designed plate impact technique; blunt tips of the isolated microcrack indicated limited stresses at the crack's tips;

2. According to the morphology and stress environment of the penny-shaped crack in Zr-BMG samples, a damaged zone similar to the cohesive zone at the rim of a penny-shaped crack is applied to characterize the crack propagation;

3. The scale of the damaged zone in this work represents the propagation scale of a penny-shaped crack. Under a given stress amplitude, the damaged zone's fast propagation would quickly bring a longer crack or cause cracks coalesce to form another longer one. The estimated

scales are reasonable compared to the micro-observations in the experiments;

4. The fact that damaged zone's fast propagation can lead to adjacent microcracks' coalescing or linking each other under a given stress amplitude is in accordance with what the critical criteria of spallation stipulated.

References

[1] D.R. Curran, L. Seaman, D.A. Shockey, Physics Reports, **147**, 5–6 (1987) 253–388

[2] F. Spaepen, Acta Metallurgica, **25**, 4 (1977) 407–415

[3] C.A. Pampillo, J. Mat. Sci. **10** (1975) 1194–1227

[4] J. Li, F. Spaepen and T.C. Hufnagel, Phil. Mag. A, **82** (2002) 2623–2630

[5] K.M. Flores, R.H. Dauskardt, Acta Mater. **49** (2001) 2527–2537.

[6] S.T. Turneaure, S.K. Dwivedi, Y.M. Gupta, J. Appl. Phys., **10**, 4 (2007) 043514

[7] J.P. Escobedo, Y.M. Gupta, J. Appl. Phys. **107**, 12 (2010) 123502

[8] X. Huang, Z. Ling, H.S. Zhang, J. Ma, L.H. Dai, J. Appl. Phys. **110**, 10 (2011) 103519

[9] Z. Ling, X. Huang, L.T. Shen, L.H. Dai, *Proceedings of DYMAT2012*, EPJ Web of Conferences **26** (2012) 02003

[10] X. Huang, Z. Ling, L.H. Dai, Int. J. Solids and Structures, **50** (2013) 1364-1372

[11] Z. Ling, X. Huang, L.H. Dai, *Hopkinson Centenary Conference Cambridge*, *UK* S.Hiermaier (eds.) (2014) 211–224

[12] X. Huang, Doctoral dissertation, University of CAS, (2013)

[13] G.I. Barenblatt, *Advances in Applied Mechanics*, H.L. Dryden, T. Von Karmen and G. Kuerti (eds.), **7** (1962)

[14] I.N. Sneddon, M. Lowengrub, *Crack problems in the Classical Theory of Elasticity* (John Wiley & Sons. Inc.1969)

[15] G.G. Chell, Engineering Fracture Mechanics, **9** (1977) 55–63

[16] J. Lu, G. Ravichandran, W.L. Johnson, Acta Mater., **51** (2003) 3429–3443

[17] F.R. Tuler, B.M. Butcher, Int. J. Fracture Mechanics, **4**, 4 (1968) 431–437